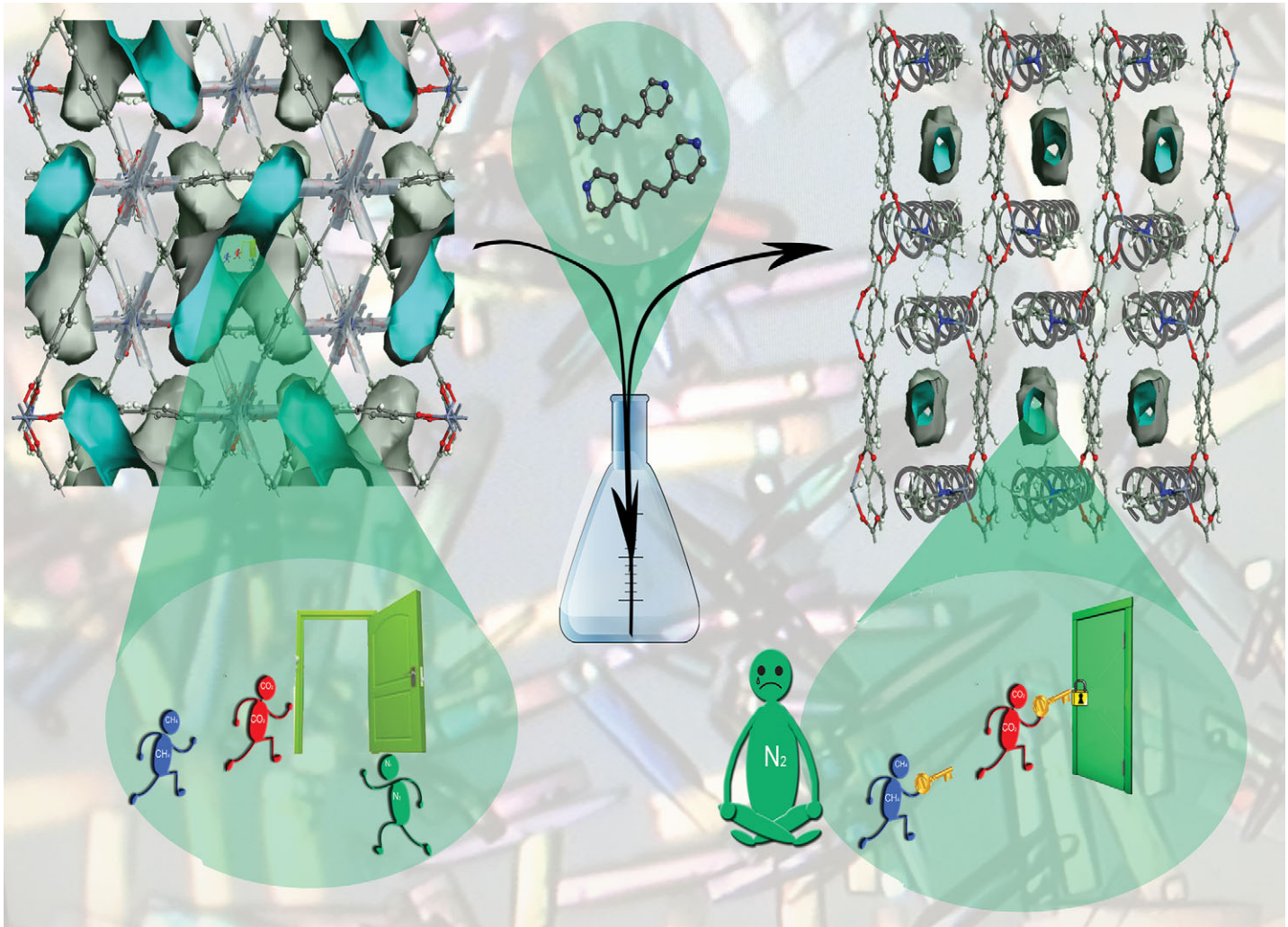

Showcasing research from the laboratory of Professor Paul A. Webley, Department of Chemical and Biomolecular Engineering, Melbourne School of Engineering, The University of Melbourne, Victoria, Australia

Converting 3D rigid metal–organic frameworks (MOFs) to 2D flexible networks *via* ligand exchange for enhanced CO_2/N_2 and CH_4/N_2 separation

A 2D novel flexible MOF was converted from a 3D rigid parent structure by ligand exchange. The incorporation of flexible heterogeneity into a rigid structure causes the substantial structural rearrangement. The daughter material efficiently excludes N_2 and exhibits enhanced CO_2/N_2 and CH_4/N_2 adsorptive separation, compared with the parent.

As featured in:

See Jin Shang, Paul A. Webley *et al.*, *Chem. Commun.*, 2015, **51**, 14716.

ROYAL SOCIETY OF CHEMISTRY

www.rsc.org/chemcomm

Registered charity number: 207890

ChemComm

COMMUNICATION

View Article Online
View Journal | View Issue

Cite this: *Chem. Commun.*, 2015, 51, 14716

Received 15th July 2015,
Accepted 31st July 2015

DOI: 10.1039/c5cc05867h

www.rsc.org/chemcomm

Converting 3D rigid metal–organic frameworks (MOFs) to 2D flexible networks *via* ligand exchange for enhanced CO_2/N_2 and CH_4/N_2 separation†

Yingdian He,[a] Jin Shang,*[ab] Qinfen Gu,[c] Gang Li,[d] Jiaye Li,[e] Ranjeet Singh,[a] Penny Xiao[ab] and Paul A. Webley*[ab]

We report a synthetic strategy for constructing a novel flexible MOF from a rigid parent structure by ligand exchange. This is the first reported study on introducing flexible heterogeneity into a rigid structure *via* substantial structural rearrangement. The daughter material exhibits enhanced gas separation selectivity compared with the parent.

Intensive studies on the development of technologies for adsorption-based gas separation have been driven worldwide by the increasing attention to the environment and the future energy demand. Adsorbents play an essential role in gas separation processes but conventional adsorbents (zeolites, activated carbon, silicon, *etc.*) are unable to meet the increasing demands placed by various industrial applications due to their limitations in structural diversity and flexibility. Novel adsorbents are required to improve gas separation performance and minimize the energy required for separation. Flexible metal–organic frameworks (MOFs) or porous coordination polymers (PCPs) are promising adsorbents for gas separation,[1] since their pore aperture and pore volume can be tuned in response to external physical, mechanical, or chemical stimuli,[2] thus achieving desired separation performance, such as high selectivity and capacity. However, the number of such flexible MOF candidates is relatively small compared with numerous rigid counterparts, because constructing phase-pure MOFs with flexible crystalline structure is difficult by typical *de novo* method.[3] Moreover, it is very challenging to rationalize the design and control of flexible moieties in the intrinsic MOF structure by direct one-pot synthesis.

Recent alternative synthesis methods, termed solvent-mediated ligand exchange[4] and solvent-assisted linker exchange (SALE),[5] provide new options for the synthesis of novel MOFs with controllable flexibility and well-defined crystallinity. Ligand exchange is typically achieved by soaking parent MOF crystals in a concentrated ligand solution. Although the understanding of this synthesis method, such as the effect of solvent, modulator, temperature, and reaction kinetics, is still in its infancy, several pioneering studies have showed considerable advantages and interesting possibilities associated with those strategies.[6] For example, solvent mediated ligand exchange was first investigated and successfully demonstrated to work for three metal–ligand coordination polymers $[Ag(L)NO_3]_\infty$, (L = pyrazine, 3,4′-bipyridine, 4,4′-pipyridine, 4-(10-(pyridin-4-yl)anthracen-9-yl)pyridine).[4] For another example, stepwise SALE has been recently reported to construct mesoporous MOFs by inserting longer pillars into the parent structure.[7] It logically follows that ligand exchange could provide a versatile strategy for producing flexible MOFs as well: by replacing rigid ligands with flexible or semi-flexible ligands, it may be possible to rationally design and construct novel flexible MOFs.

Herein, we report the conversion of a three-dimensional (3D) rigid framework MOF by ligand exchange into a novel two-dimensional (2D) flexible network whose pure-phase sample could not be obtained by direct synthesis in spite of many attempts in our lab. To the best of our knowledge, it is the first case of incorporating an exotic flexible-ligand into a rigid pillar-layered MOF structure *via* structural rearrangement during ligand exchange, creating structural flexibility in the daughter material. Interestingly, the adsorption properties of the daughter material suggest a superior gas separation performance to the parent material. The solvo-thermal reaction of $Zn(CH_3COO)_2 \cdot 2H_2O$, H_2BPDC (BPDC = 4,4′-biphenyldicarboxylate) and BiPY (BiPY = 4,4′-bipyridine) produced colourless parent crystals **1**.‡ Using **1** as precursor, the daughter material **2** was obtained by simply immersing **1** in a concentrated fresh 1,3-bis(4-pyridyl)-propane (BPP) solution at 105 °C without stirring for four

[a] *Department of Chemical and Biomolecular Engineering, The University of Melbourne, Victoria 3010, Australia. E-mail: jin.shang@unimelb.edu.au, paul.webley@unimelb.edu.au; Tel: +61-3-90357873*
[b] *Cooperative Research Center for Greenhouse Gas Technologies (CO2CRC), Melbourne, Australia*
[c] *Australian Synchrotron, 800 Blackburn Rd, Clayton, Victoria 3168, Australia*
[d] *Australian Centre for Energy, School of Mechanical and Chemical Engineering, The University of Western Australia, Crawley, WA 6009, Australia*
[e] *School of Chemistry, Monash University, Victoria 3800, Australia*

† Electronic supplementary information (ESI) available: Experimental details, techniques, crystal data. CCDC 1404865. For ESI and crystallographic data in CIF or other electronic format see DOI: 10.1039/c5cc05867h

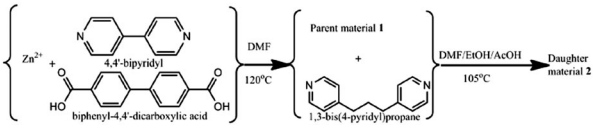

Scheme 1 Synthesis route of parent **1** and daughter **2** samples.

consecutive 3-day exchanges (Scheme 1). A detailed synthesis is provided in ESI.† Interestingly, a complete structural rearrangement occurred, with an entirely distinct pure-phase structure produced, as confirmed by synchrotron powder X-ray diffraction (PXRD) (Fig. 1). Specifically, the structure transferred from Orthorhombic (*Pbcn*) to Monoclinic ($P2_1/c$) with unit cell parameters provided in Table S1, ESI.† As shown in ESI,† Fig. S1, the crystal structure of the parent sample **1** consists of trinuclear Zn clusters which are connected to the carboxylate groups of six BPDC bridging linkers to form 2D double layers; and the secondary ligands BiPY, as pillars, support the 2D layers to generate a 3D framework. The structure of **1** is similar to those reported,[8] in spite of the variance in reaction temperature and metal source in this work compared with the reported synthetic procedure, indicating the favoured coordination state in the system. In contrast, the daughter structure **2** exhibits a completely distinct crystallographic structure. Two oxygen atoms from the carboxylate group of two different BPDC are coordinated to one Zn centre, and the chains are connected by the Zn–N bond of the BPP whose N-to-N distance is approximately 8.5 Å. Thus, in this coordination system, BPP is expected to approach maximum stretching of the GG′ conformation which displays an N–N distance from 6.7 to 8.6 Å.[9] The various conformations, due to the flexibility of the $-(CH_2)_3-$ chain and the rotation of pyridyl rings, would be essential to the complete ligand exchange reaction. As seen from Fig. 2d, a buckled layer consists of two tangled networks (blue and red colours) in the *ac* plane; these buckled layers are then stacked up in the order of *ababa* along the *b*-axis. The daughter material exhibits a 2D flexible structure derived from both the unique topology and the bridging ligands, as further characterized below. To the best of our knowledge, it represents a rare example of 3D to 2D transformation during ligand replacement or desolvation, among the very large family of numerous MOFs.[10]

Thermal gravimetric analysis (TGA) indicated **2** is thermally stable up to 316 °C in N_2 atmosphere (ESI,† Fig. S2). The weight

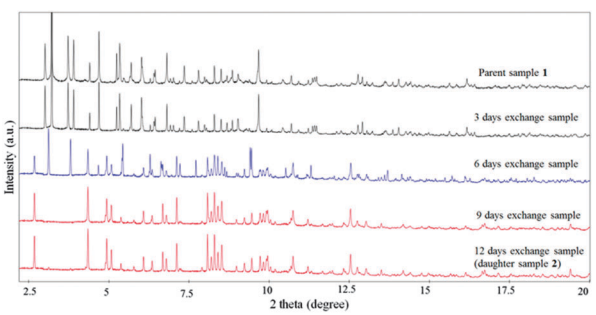

Fig. 1 Synchrotron powder XRD of as-made parent **1** and samples with 3, 6, 9, and 12 days exchange time.

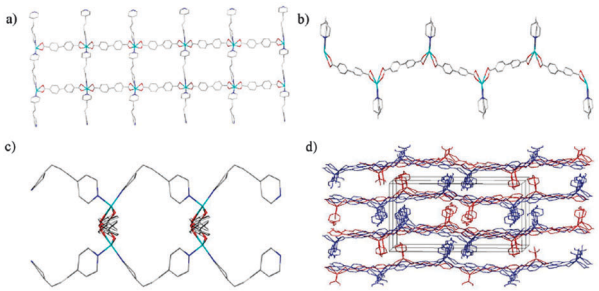

Fig. 2 Two-dimensional layer structure of daughter material **2**: (a) view down crystallographic *b* axis; (b) view down crystallographic *a* axis; (c) view down crystallographic *c* axis; (d) unit cell of 2 × 1 × 1. Colour scheme: Zn (cyan), C (grey), O (red), N (blue).

loss steps for the decomposition of BiPY of **1** and BPP of **2** occurred approximately at 372 and 318 °C, respectively. To better understand the mechanism of structure conversion from **1** to **2**, we conducted synchrotron PXRD for samples collected at different reaction times: 3, 6, 9, and 12 days, to monitor the crystal phase transformation during the ligand exchange process. (Fig. 1) The parent crystal structure remained unchanged after 3 days exchange, and after 9 days, a new crystal phase of daughter material **2** formed. It is interesting that a heterogeneous product (approximately 40.1 wt% of **1** and 59.9 wt% of **2**) was obtained for the 6 days sample, which may be indicative of a core–shell structure- this needs to be confirmed through more comprehensive microscopic characterisation. (ESI,† Plot S2) From the liquid ^{1}H NMR analysis, the BiPY ligands in the parent material were completely replaced by BPP in the daughter material (ESI,† Fig. S3–S7). Scanning electron microscope (SEM) images show that the single crystals of parent sample **1** cracked into meso-crystals to form the structure of the daughter material **2**, (ESI,† Fig. S8 and S9) rather than the single-crystal to single-crystal (SCSC) transformation which is usually observed during ligand exchange.[11]

Although several pioneering studies explored the chemical principles behind ligand exchange,[12] the reaction mechanism in a certain coordination system is complicated and at present cannot be predicted a priori. In our case, acetic acid might act as a catalyst to promote the ligand exchange.[13] The solvent-mediated reaction logically starts at the external surface of the parent crystals, and progresses into the inner structure. In addition, the stable secondary building unit (SBU) of the parent structure would experience disassembly, thus the underlying mechanism to undergo ligand exchange through the surface of the crystal is likely to be a dissolution/recrystallization process. As one of the family of pillared-paddlewheel MOFs, it is well known that the Zn–O bonds are significantly stronger than the Zn–N bonds,[5,14] which enables the ligand exchange to occur by Zn–N bond cleavage and reforming involved in N-contained ligands rather than carboxylate ligands. Therefore, the topologies of the parent samples are sustained. However, the substantial structural arrangement observed in our work can be attributed to solvent-mediated ligand exchange (in contrast to a solid-state transformation), namely, the dissolution and recrystallization

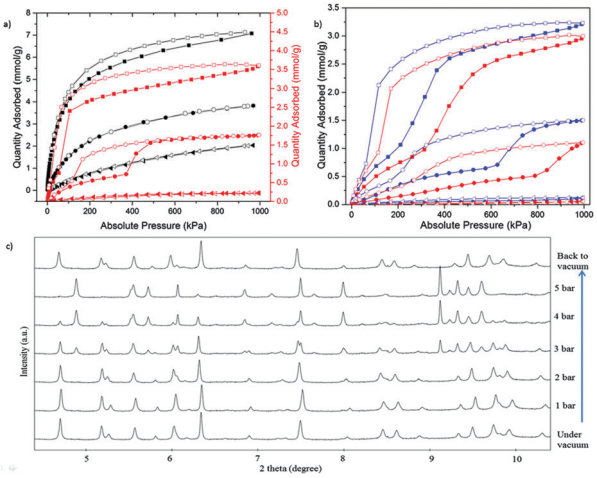

Fig. 3 (a) CO_2, CH_4, N_2 adsorption/desorption isotherms of **1** and **2** at 273 K (note different *Y* axis for **1** (in black) left and **2** (in red) right are presented for clarity); (b) CO_2, CH_4, and N_2 adsorption/desorption isotherms of **2** at 298 K (in blue) and 313 K (in red); (c) *in situ* synchrotron PXRD of **2** depending on CO_2 pressure at 298 K. (In a and b, solid: adsorption; open: desorption; left-triangle N_2, diamond H_2, square CO_2, circle CH_4; lines are guide to the eye.)

mechanism as described in the literature.[4,15] The oxygen from deprotonated acetic acid may temporarily replace carboxylate oxygen and coordinate to the Zn ion, which promotes the disassembly of the parent metal cluster. Subsequently, the carboxylate ligands replace the oxygen of acetate acid, and BPP replaces BiPY completely to form a favourable topology *via* structural rearrangement.

Importantly, the daughter material **2** exhibits guest molecule induced transformation from non-porous to porous structures. At 77 K and 1 bar, **1** adsorbs a substantial amount of N_2 and H_2: 12.0 and 9.4 mmol g^{-1}, respectively (ESI,† Fig. S10). In striking contrast, the adsorption capacity of N_2 and H_2 on **2** were negligible under the same conditions, indicative of a non-porous crystal state. Hence, the conversion of the parent 3D structure to the daughter 2D structure would be beneficial to gas separation by excluding certain gases. Interestingly, CO_2 and CH_4 sorption on **2** up to 10 bar at 273, 298 and 313 K (Fig. 3a and b), show the typical isotherms for flexible MOFs – obvious adsorption steps with large hysteresis,[16] which indicates structural flexibility and crystal phase transition upon gas sorption. To confirm the reversible structural transformation, we conducted *in situ* synchrotron PXRD depending on CO_2 pressure. As shown in Fig. 3c, main peaks of the PXRD patterns of **2** shifted reversibly when the sample was under vacuum or various CO_2 pressures, and the CO_2 transition pressure is consistent with the step isotherm at 298 K (Fig. 3b). The adsorbate-induced structural transformations occurring in the case of CO_2 and CH_4 are attributed to strong interaction between gas molecules and the crystal, due to the relatively large quadrupole moment for CO_2 of -1.43×10^{-39} C m^2 *vs.* N_2 of -4.7×10^{-40} C m^2, and polarizability for CH_4 (25.9×10^{-25} cm^{-3} *vs.* N_2 of 17.4×10^{-25} cm^{-3}). In other words, upon CO_2 and CH_4 adsorption, the non-porous desolvated **2** structure transformed to a porous network at the transition pressure, implying superior gas separation properties to the parent material **1**. In contrast, the N_2 adsorption amount is negligible up to 10 bar on **2** due to the weak adsorbate–adsorbent interactions, resulting in considerably enhanced CO_2/N_2 and CH_4/N_2 selectivity, compared with those for the parent material. Specifically, the daughter material exhibits ideal selectivity of CO_2/N_2 of 80 at 1 bar at 273 K based on pure component adsorption, compared with 8 for the parent sample. With regard to the CH_4/N_2 selectivity, the value increased from 1.86 to 8.2 at 10 bar at 273 K, which is comparable to the highest numbers in the open literature[17] and holds promise for recovering CH_4 from low-grade natural gas.

In conclusion, we report a novel route to convert a 3D rigid MOF structure to a 2D flexible network and the latter one shows reversible transformation from a non-porous to porous structure as induced by certain guest molecules, exhibiting a superior gas separation potential. We propose that the synthetic strategy can be potentially generalized and applied to other pillar-layered MOFs structures. This work provides more information on interpretation of substantial structural rearrangement *via* ligand exchange. Further investigations on the applicability of the synthetic methodology to other MOFs families are in progress.

Y.H. acknowledges the Chinese Scholarship Council (CSC). P.A.W. and J.S. acknowledge Australian Research Council (ARC) for providing the funding (DP2013000024). G.L. is a recipient of ARC DECRA (DE140101824). Part of work was undertaken on the PD beamline, Australian Synchrotron.

Notes and references

‡ Crystal structure of parent sample **1** can refer to the previous reported structure (CCDC 192723). Crystal Structure of daughter material **2** (CCDC 1404865) was determined based on synchrotron powder XRD data, and detailed information is provided in ESI.† The formulae of the parent material **1** and daughter material **2** are $[Zn_3(C_{14}H_8O_4)_3(C_{10}H_8N_2)]$ solvent and $[Zn(C_{14}H_8O_4)(C_{13}H_{14}N_2)]$ solvent, respectively.

1 (*a*) S. S. Nagarkar, A. V. Desai and S. K. Ghosh, *Chem. – Asian J.*, 2014, **9**, 2358–2376; (*b*) J. R. Li, J. Sculley and H. C. Zhou, *Chem. Rev.*, 2012, **112**, 869–932; (*c*) H. Furukawa, K. E. Cordova, M. O'Keeffe and O. M. Yaghi, *Science*, 2013, **341**, 1230444.
2 (*a*) R. Lyndon, K. Konstas, B. P. Ladewig, P. D. Southon, P. C. J. Kepert and M. R. Hill, *Angew. Chem., Int. Ed.*, 2013, 3695–3698; (*b*) N. Yanai, T. Uemura, M. Inoue, R. Matsuda, T. Fukushima, M. Tsujimoto, S. Isoda and S. Kitagawa, *J. Am. Chem. Soc.*, 2012, **134**, 4501–4504.
3 (*a*) C. R. Murdock, B. C. Hughes, Z. Lu and D. M. Jenkins, *Coord. Chem. Rev.*, 2014, **258–259**, 119–136; (*b*) A. Schneemann, V. Bon, I. Schwedler, I. Senkovska, S. Kaskel and R. A. Fischer, *Chem. Soc. Rev.*, 2014, **43**, 6062–6096.
4 X. Cui, A. N. Khlobystov, X. Chen, D. H. Marsh, A. J. Blake, W. Lewis, N. R. Champness, C. J. Roberts and M. Schröder, *Chem. – Eur. J.*, 2009, **15**, 8861–8873.
5 O. Karagiaridi, W. Bury, J. E. Mondloch, J. T. Hupp and O. K. Farha, *Angew. Chem., Int. Ed. Engl.*, 2014, **53**, 4530–4540.
6 P. Deria, J. E. Mondloch, O. Karagiaridi, W. Bury, J. T. Hupp and O. K. Farha, *Chem. Soc. Rev.*, 2014, **43**, 5896–5912.
7 O. Karagiaridi, W. Bury, E. Tylianakis, A. A. Sarjeant, J. T. Hupp and O. K. Farha, *Chem. Mater.*, 2013, **25**, 3499–3503.
8 Q. Fang, X. Shi, G. Wu, G. Tian, G. Zhu, R. Wang and S. Qiu, *J. Solid State Chem.*, 2003, **176**, 1–4.
9 L. Carlucci, G. Ciani, D. M. Proserpio and S. Rizzato, *CrystEngComm*, 2002, **4**, 121.
10 (*a*) L.-J. Dong, C.-C. Zhao, X. Xu, Z.-Y. Du, Y.-R. Xie and J. Zhang, *Cryst. Growth Des.*, 2012, **12**, 2052–2058; (*b*) Y. Kim, J. H. Song,

W. R. Lee, W. J. Phang, K. S. Lim and C. S. Hong, *Cryst. Growth Des.*, 2014, **14**, 1933–1937.
11 T. Li, M. T. Kozlowski, E. A. Doud, M. N. Blakely and N. L. Rosi, *J. Am. Chem. Soc.*, 2013, **135**, 11688–11691.
12 (*a*) A. F. Gross, E. Sherman, S. L. Mahoney and J. J. Vajo, *J. Phys. Chem. A*, 2013, **117**, 3771–3776; (*b*) M. Kim, J. F. Cahill, Y. Su, K. A. Prather and S. M. Cohen, *Chem. Sci.*, 2012, **3**, 126–130; (*c*) O. Karagiaridi, M. B. Lalonde, W. Bury, A. A. Sarjeant, O. K. Farha and J. T. Hupp, *J. Am. Chem. Soc.*, 2012, **134**, 18790–18796.
13 M. Kim, J. F. Cahill, H. Fei, K. A. Prather and S. M. Cohen, *J. Am. Chem. Soc.*, 2012, **134**, 18082–18088.
14 S. Bureekaew, S. Amirjalayer and R. Schmid, *J. Mater. Chem.*, 2012, **22**, 10249.
15 (*a*) A. N. Khlobystov, N. R. Champness, C. J. Roberts, S. J. Tendler, C. Thompson and M. Schröder, *CrystEngComm*, 2002, **4**, 426–431; (*b*) F. Pan, J. Wu, H. Hou and Y. Fan, *Cryst. Growth Des.*, 2010, **10**, 3835–3837.
16 S. Horike, S. Shimomura and S. Kitagawa, *Nat. Chem.*, 2009, **1**, 695–704.
17 X. Ren, T. Sun, J. Hu and S. Wang, *RSC Adv.*, 2014, **4**, 42326–42336.